



Supplement of

Satellite observations reveal 13 years of reservoir filling strategies, operating rules, and hydrological alterations in the Upper Mekong River basin

Dung Trung Vu et al.

Correspondence to: Stefano Galelli (stefano_galelli@sutd.edu.sg)

The copyright of individual parts of the supplement might differ from the article licence.

Text S1. Commonalities and differences between our study and the Mekong Dam Monitor

Both our study and the Mekong Dam Monitor (MDM) are based on the idea of extracting the water extent of the reservoirs from satellite images and then converting it into water level and storage by using the information from a Digital Elevation Model (DEM). However, there are a few key differences. First, we use an image improvement algorithm, which is important and necessary because it enables us to extract the information on reservoir storage from Landsat images for a long period (2008–2020). Meanwhile, to avoid the cloud contamination in satellite images, MDM looks to other remote sensing products, such as the Sentinel-SAR (Synthetic Aperture Radar), which can “pierce” through clouds. However, Sentinels were launched recently (in April 2014), so the information before that time (including the construction and filling periods of five reservoirs on the mainstream of the Lancang) cannot be revealed. Second, with the water extent estimation provided by our algorithm, we directly infer water level and storage through the elevation-area-storage curves estimated from the DEM. Meanwhile, MDM calculates the average elevation at the reservoir shoreline, and then converts it into storage. This way may not work well for all water surface images. Finally, to strengthen our results, we make use of water level from Altimetry data (where available) to validate the results obtained by processing the Landsat images.

Table S1. Design specifications of the hydropower dams on the mainstream of the Lancang River. Retrieved from Do et al. (2020).

Name	Year of Commission	Dam Height (m)	Max WL (m a.s.l.)	Dead WL (m a.s.l.)	Max WSA (km ²)	Dead Storage (MCM)	Full Storage (MCM)	Hydropower Capacity (MW)
Jinghong	2009	108	602	595	510	810	1119	1750
Nuozhadu	2014	262	812	756	320	10414	21749	5850
Dachaoshan	2003	115	899	887	826	465	740	1350
Manwan	1992	132	994	982	415	630	887	1670
Xiaowan	2010	292	1236	1162	194	4750	14645	4200
Gongguoqiao	2012	105	1319	1311	343	196	316	900
Miaowei	2016	140	1408	1373	171	359	660	1400
Dahuaqiao	2018	106	1477	1466	148	252	293	920
Huangdeng	2017	203	1619	1604	199	1031	1418	1900
Tuoba	2023	158	1735	1725	177	735	1039	1400
Lidi	2019	74	1818	1813	4	57	71	420
Wunonglong	2018	138	1906	1894	163	236	272	990

WL Water level

WSA Water surface area

Table S2. Specifications of Landsat, MODIS and Sentinel images.

Satellite	Landsat (NASA and USGS)				MODIS	Sentinel (ESA)		
	1-3	4-5	7	8	(NASA)	1	2	3
First Launch	1972	1982	1999	2013	1999	2014	2015	2016
Instrument	MSS	MSS, TM	ETM+	OLI, TIRS	MODIS	SAR	MSI	OLCI
Best Resolution	60 m	30 m	30 m	30 m	250 m	5 m	10 m	300 m
Frequency (Day)	16	16	16	16	1	12	10	27
Cloud Cover	Yes	Yes	Yes	Yes	Yes	No	Yes	Yes

MODIS Moderate Resolution Imaging Spectroradiometer

USGS United States Geological Survey

ESA European Space Agency

MSS Multi Spectral Scanner

TM Thematic Mapper

ETM+ Enhanced Thematic Mapper Plus

OLI Operational Land Imager

TIRS Thermal Infrared Sensor

SAR Synthetic Aperture Rada

MSI Multi-Spectral Instrument

OLCI Ocean and Land Colour Instrumen

Table S3. Specifications of satellite altimeters.

Satellite	Type	Organization	Operation Time	Repeat Period (day)
Topex/Poseidon	Radar	NASA and CNES	1992-2002	10
Jason 1	Radar	NASA and CNES	2002-2008	10
Jason 2	Radar	NASA and CNES	2008-2016	10
Jason 3	Radar	NASA and CNES	2016-current	10
ERS 1	Radar	ESA	1992-1996	35
ERS 2	Radar	ESA	1996-2003	35
Envisat	Radar	ESA	2002-2010	35
SARAL	Radar	ISRO and CNES	2013-2016	35
Sentinel 3A	Radar	ESA	2016-current	27
Sentinel 3B	Radar	ESA	2018-current	27
ICESat 1	Laser	NASA	2003-2009	91
ICESat 2	Laser	NASA	2018-current	91

CNES National Centre for Space Studies
ESA European Space Agency
ISRO Indian Space Research Organization

ERS European Remote Sensing
SARAL Satellite with ARGOS and ALtika
ICESat Ice, Cloud, and land Elevation Satellite

Table S4. The differences in storage corresponding to each water level in the variation range of Nuozhadu and Xiaowan reservoirs obtained by using the trapezoidal approximation [1] and direct calculation from the DEM [2].

Nuozhadu				Xiaowan							
Water Level (m)	Storage [1] (MCM)	Storage [2] (MCM)	Difference (%)	Water Level (m)	Storage [1] (MCM)	Storage [2] (MCM)	Difference (%)	Water Level (m)	Storage [1] (MCM)	Storage [2] (MCM)	Difference (%)
766	10501	10678	1.67	1162	4077	4149	1.74	1210	9112	9251	1.50
768	10859	11042	1.65	1164	4223	4298	1.74	1212	9392	9534	1.49
770	11227	11414	1.64	1166	4375	4452	1.73	1214	9678	9823	1.47
772	11605	11797	1.63	1168	4531	4611	1.74	1216	9970	10118	1.46
774	11992	12189	1.62	1170	4693	4776	1.74	1218	10268	10419	1.45
776	12390	12592	1.61	1172	4862	4948	1.74	1220	10572	10726	1.44
778	12798	13005	1.59	1174	5036	5126	1.74	1222	10882	11039	1.42
780	13216	13428	1.58	1176	5217	5309	1.74	1224	11198	11358	1.41
782	13645	13862	1.57	1178	5403	5498	1.73	1226	11521	11684	1.40
784	14084	14307	1.56	1180	5595	5692	1.71	1228	11849	12015	1.38
786	14534	14763	1.55	1182	5792	5892	1.70	1230	12184	12353	1.37
788	14995	15230	1.54	1184	5994	6096	1.68	1232	12525	12697	1.36
790	15468	15709	1.53	1186	6201	6306	1.67	1234	12872	13047	1.35
792	15953	16199	1.52	1188	6413	6520	1.65	1236	13225	13404	1.33
794	16450	16702	1.51	1190	6630	6741	1.64	1238	13584	13766	1.32
796	16958	17217	1.50	1192	6853	6966	1.62	1240	13950	14134	1.30
798	17479	17743	1.49	1194	7081	7197	1.61	1242	14321	14508	1.29
800	18012	18283	1.48	1196	7316	7434	1.60				
802	18557	18834	1.47	1198	7555	7677	1.59				
804	19115	19399	1.46	1200	7801	7925	1.57				
806	19686	19975	1.45	1202	8052	8179	1.56				
808	20269	20565	1.44	1204	8308	8438	1.54				
810	20865	21167	1.43	1206	8570	8703	1.53				
812	21473	21781	1.42	1208	8838	8974	1.51				

Table S5. Spectral indices for water surface extraction.

Index	Formula	Recommended Threshold Values
NDVI	$(\text{Red}-\text{Green})/(\text{Red}+\text{Green})$	0 (Zhai et al., 2015) and 0.1 (Gao et al., 2012)
NDWI	$(\text{Green}-\text{NIR})/(\text{Green}+\text{NIR})$	0 (Zhai et al., 2015), (Bonnema and Hossain, 2017)
MNDWI	$(\text{Green}-\text{MIR})/(\text{Green}+\text{MIR})$	0 and 0.1 (Duan and Bastiaanssen, 2013)

NDVI Normalized Difference Vegetation Index
NDWI Normalized Difference Water Index
MNDWI Modified Normalized Difference Water Index

NIR Near Infrared
MIR Middle Infrared

Table S6. Performance of the water surface area estimation algorithm for the reservoirs on the Lancang River.

Dry season (Dec-May)			
Reservoir	Number of Available Images	Percentage of Usable Images	
		Before Improvement	After Improvement
Jinghong	175	24%	89%
Nuozhadu	187	27%	89%
Dachaoshan	187	26%	89%
Manwan	187	25%	85%
Xiaowan	187	27%	88%
Gongguoqiao	173	34%	75%
Miaowei	173	36%	84%
Dahuaqiao	173	36%	82%
Huangdeng	164	34%	85%
Wunonglong	164	34%	73%
Total	1770	30%	84%

Wet season (Jun-Nov)			
Reservoir	Number of Available Images	Percentage of Usable Images	
		Before Improvement	After Improvement
Jinghong	122	20%	80%
Nuozhadu	127	13%	69%
Dachaoshan	130	16%	76%
Manwan	131	18%	77%
Xiaowan	130	16%	88%
Gongguoqiao	118	23%	69%
Miaowei	118	27%	90%
Dahuaqiao	118	28%	81%
Huangdeng	120	27%	78%
Wunonglong	120	20%	81%
Total	1234	21%	79%

Total			
Reservoir	Number of Available Images	Percentage of Usable Images	
		Before Improvement	After Improvement
Jinghong	297	22%	85%
Nuozhadu	314	21%	81%
Dachaoshan	317	22%	84%
Manwan	318	22%	82%
Xiaowan	317	23%	88%
Gongguoqiao	291	29%	72%
Miaowei	291	32%	87%
Dahuaqiao	291	33%	81%
Huangdeng	284	31%	82%
Wunonglong	284	28%	76%
Total	3004	26%	82%

Table S7. Quantitative comparison of Landsat-derived and altimetry-converted water surface area.

Reservoir	R (CC)	RMSE (km ²)	NRMSE
Nuozhadu	0.994	13.941	0.049
Xiaowan	0.977	9.901	0.062
Huangdeng	0.977	1.884	0.077
Jinghong	0.558	0.428	0.020

Table S8. The statistical indices of the annual peak and lowest discharge at Chiang Saen station for two periods: before and after the two biggest dams (Nuozhadu and Xiaowan) began operations.

	Peak Discharge (cms)				Lowest Discharge (cms)			
	Mean	Q1	Median	Q3	Mean	Q1	Median	Q3
1990 - 2008	11157	9235	10700	12350	638	551	599	759
2013 - 2020	6476	5213	6834	7866	966	844	975	1077
Change	-45%	-45%	-43%	-42%	57%	69%	65%	42%

Figure S1. Comparison between Landsat-derived water level (green line), Jason altimetry water level (blue dots), and Sentinel-1-derived water level (orange dashed line) archived from Mekong Dam Monitor Platform for Nuozhadu (left) and Xiaowan (right) reservoirs. Note that Jason has a 10-day temporal resolution and Sentinel-1 have a frequency of up to 6 days (Sentinel-1A and B have a frequency of 12 days and interleave to each other). The comparison shows that the use of a monthly resolution yields the same trajectories of a weekly one.

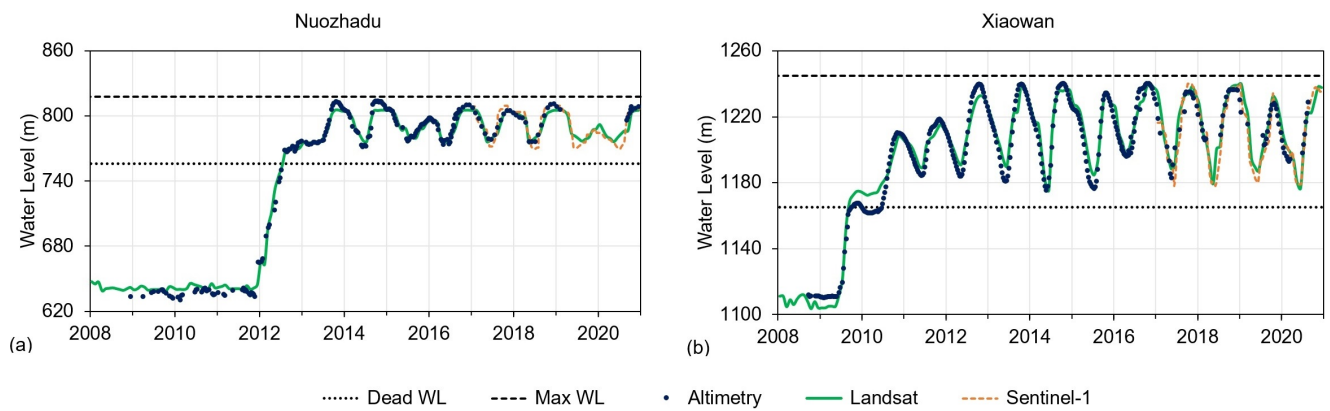


Figure S2. E-A, A-S, and E-S curves of Bhumibol reservoir (top) and Ubol Ratana reservoir (bottom). The curves are represented by light blue lines, which are fitted to the data points (blue circles) derived from the DEM data. Note that the curves intersect the points identified by maximum water level, maximum water surface area, and full storage volume (dashed lines) as well as those identified by dead water level and dead storage volume (dotted lines). The green lines reported in panels (c) and (f) correspond to the observations by Electricity Generating Authority of Thailand (EGAT).

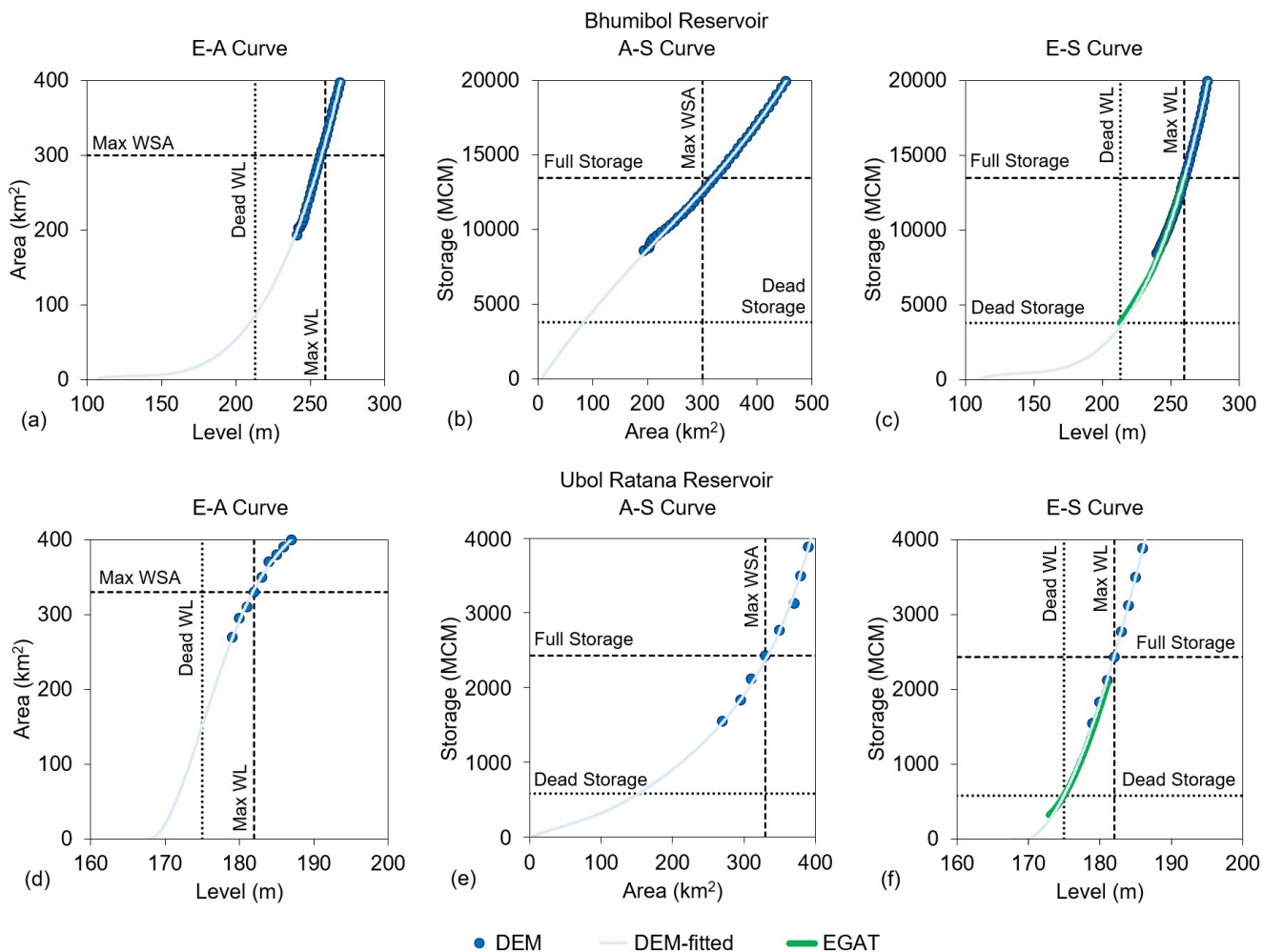


Figure S3. Water surface area (a,b) and storage variations (c,d) of Bhumibol reservoir (left) and Ubol Ratana reservoir (right). In panels (a,b), note the drastic difference in WSA values before (light blue points) and after (cyan points) the classification improvement. The corrected values of WSA are well in agreement with those converted from observed water level (EGAT) through E-A curves (blue dashed lines). In panels (c,d), note the similarity in the storage volume derived from Landsat images (cyan dotted lines) and observed data from EGAT (blue lines).

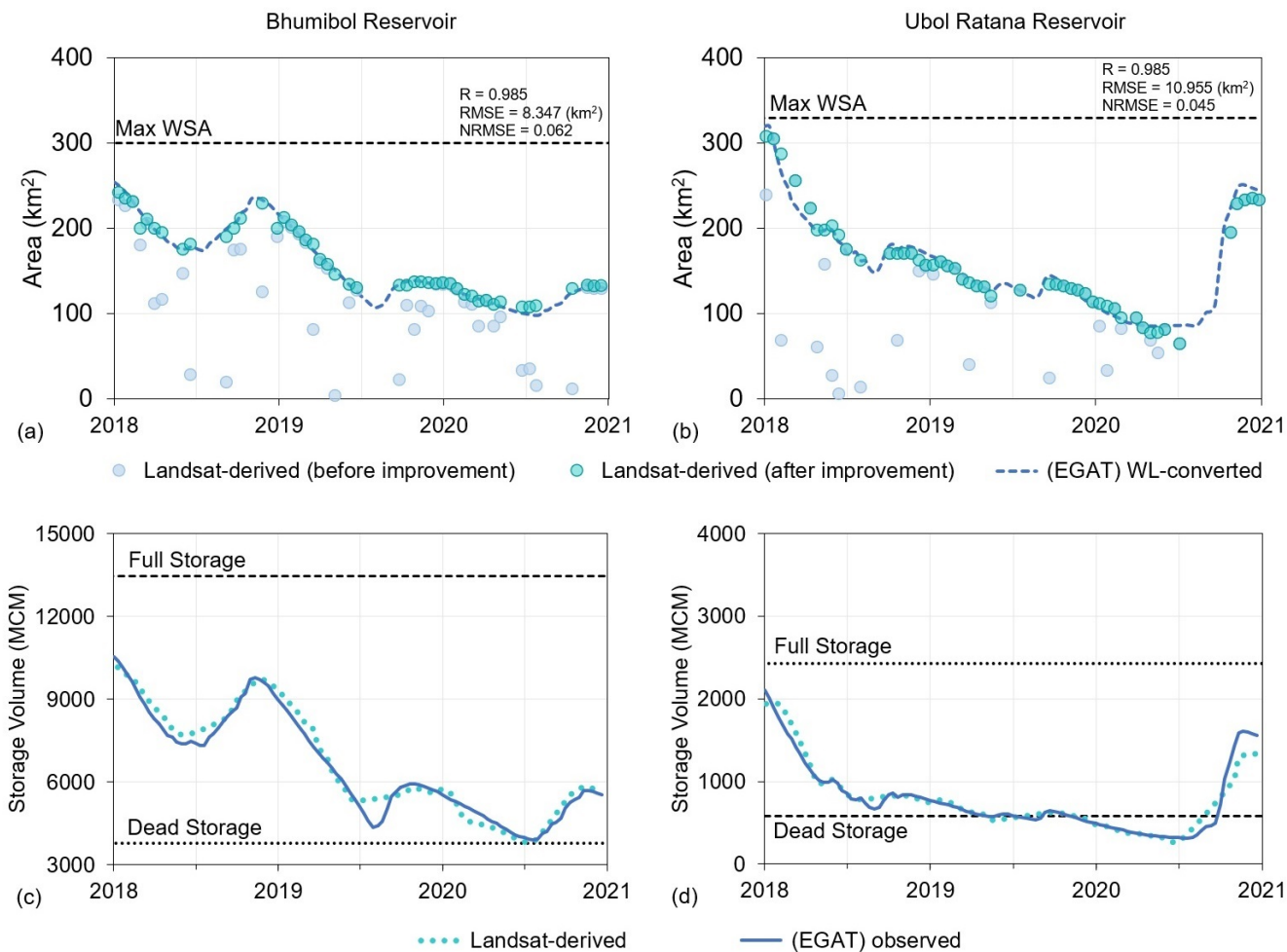


Figure S4. E-S curve of Nouzhadu (left) and Xiaowan (right) reservoirs obtained by using the trapezoidal approximation and direct calculation from the DEM.

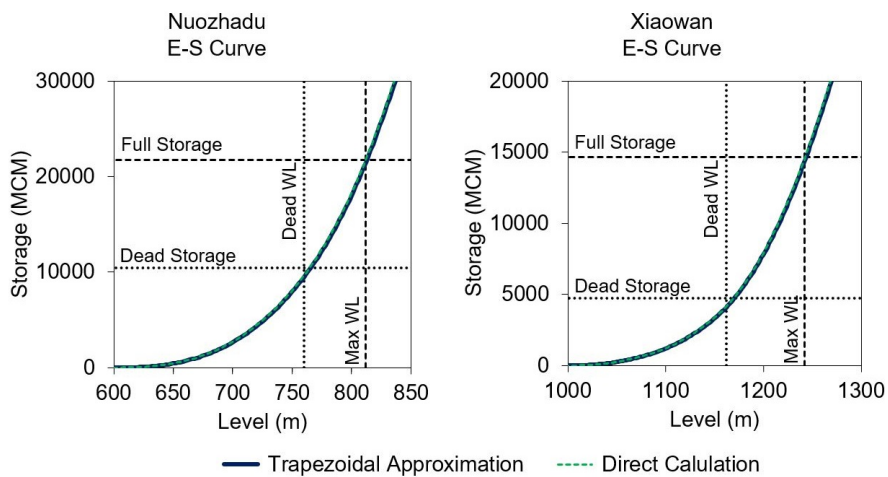


Figure S5. Performance of three spectral indices (NDVI, NDWI, and MNDWI) in extracting the water surface area of Nuozhadu reservoir. Results are reported for three threshold values, 0, 0.05, and 0.1 and compared to the Maximum Water Extent dataset, developed by the European Commission’s Joint Research Centre (Pekel et al., 2016). The meaning of the three indices is explained in Table S5.

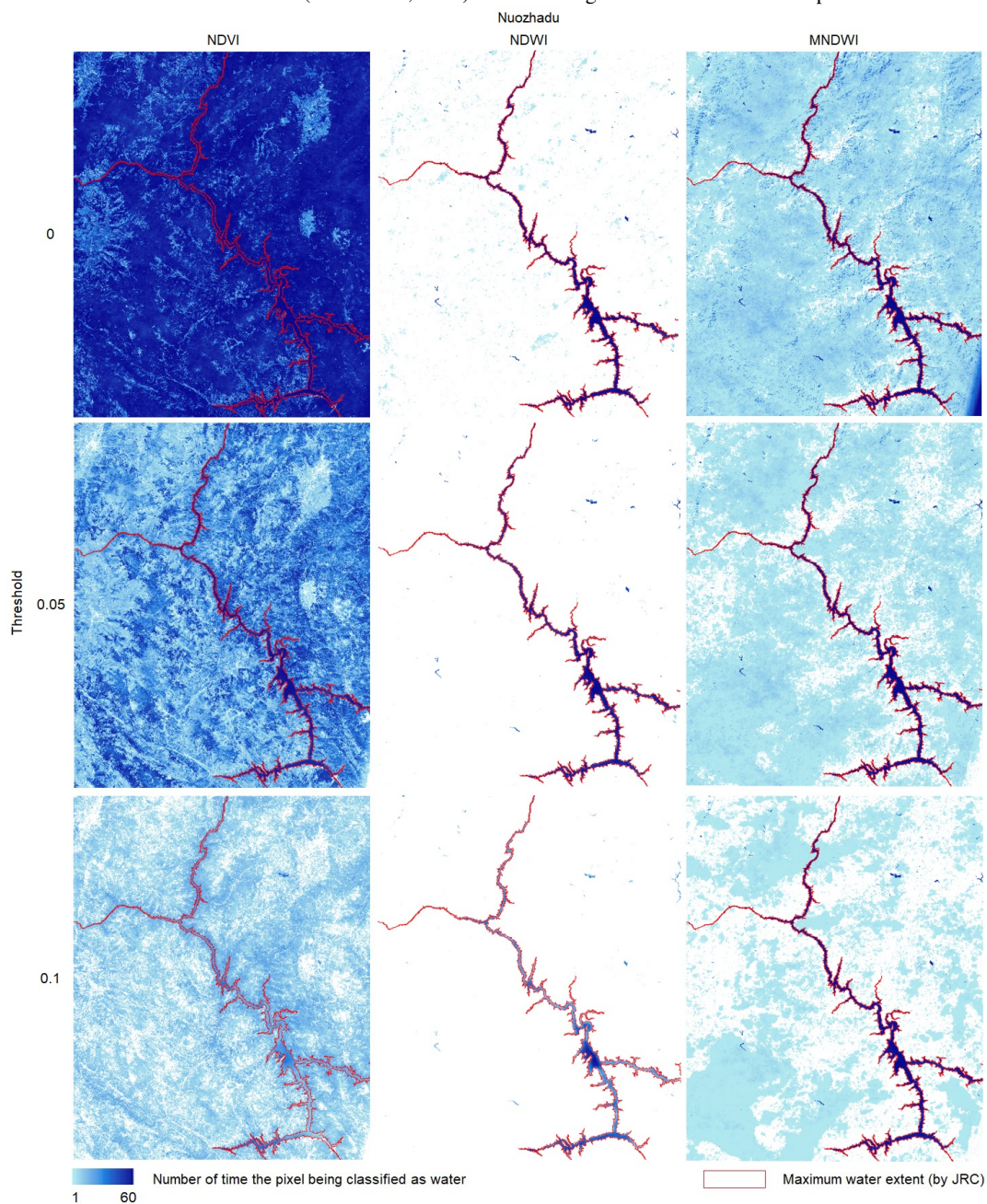


Figure S6. Performance of three spectral indices (NDVI, NDWI, and MNDWI) in extracting the water surface area of Xiaowan (top) and Manwan (bottom) reservoirs. Results are reported for three threshold values, 0, 0.05, and 0.1 and compared to the Maximum Water Extent dataset, developed by the European Commission’s Joint Research Centre (Pekel et al., 2016). The meaning of the three indices is explained in Table S5.

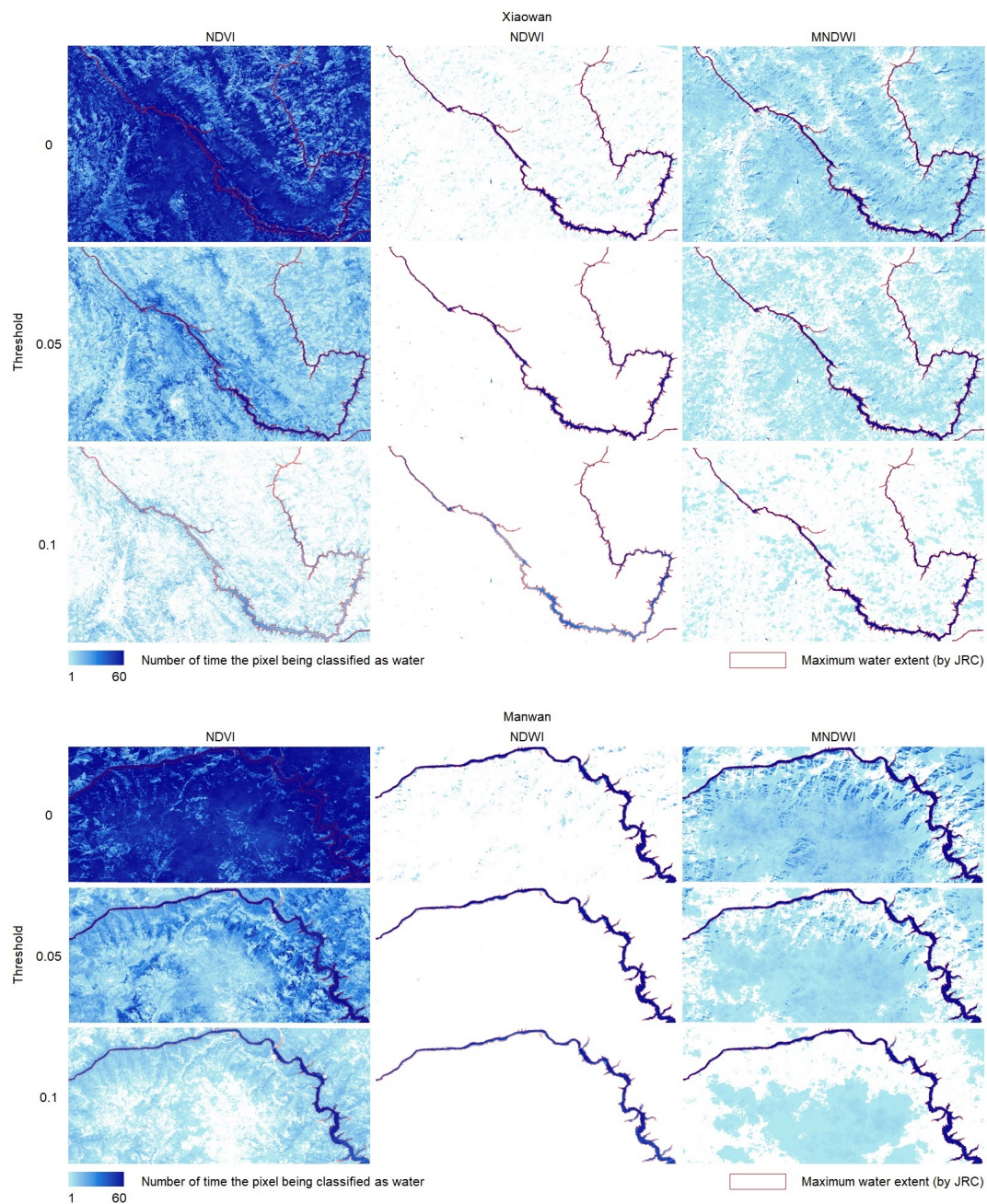


Figure S7. Performance of three spectral indices (NDVI, NDWI, and MNDWI) in extracting the water surface area of Jinghong (left) and Dachaoshan (right) reservoirs. Results are reported for three threshold values, 0, 0.05, and 0.1 and compared to the Maximum Water Extent dataset, developed by the European Commission’s Joint Research Centre (Pekel et al., 2016). The meaning of the three indices is explained in Table S5.

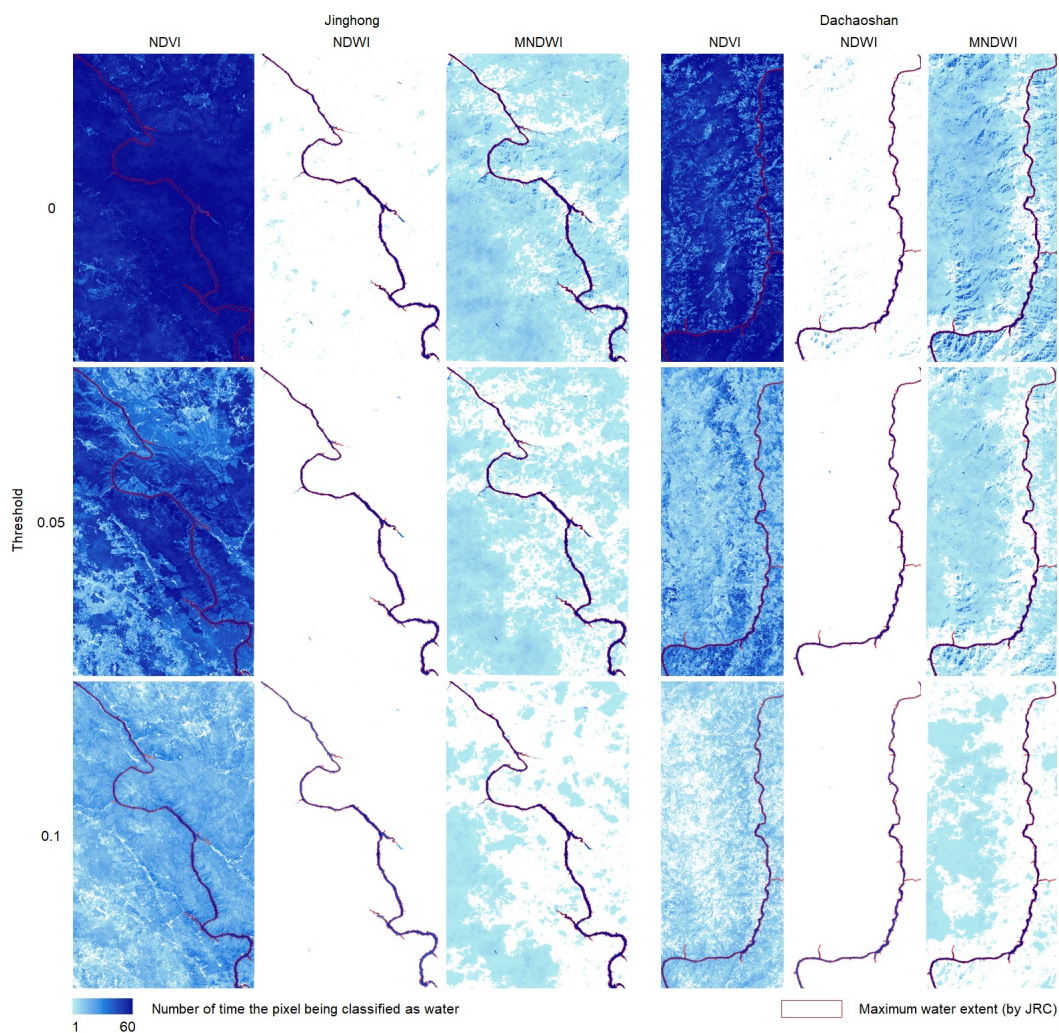


Figure S8. Performance of three spectral indices (NDVI, NDWI, and MNDWI) in extracting the water surface area of Gongguoqiao (left) and Dahuaqiao (right) reservoirs. Results are reported for three threshold values, 0, 0.05, and 0.1 and compared to the Maximum Water Extent dataset, developed by the European Commission’s Joint Research Centre (Pekel et al., 2016). The meaning of the three indices is explained in Table S5.

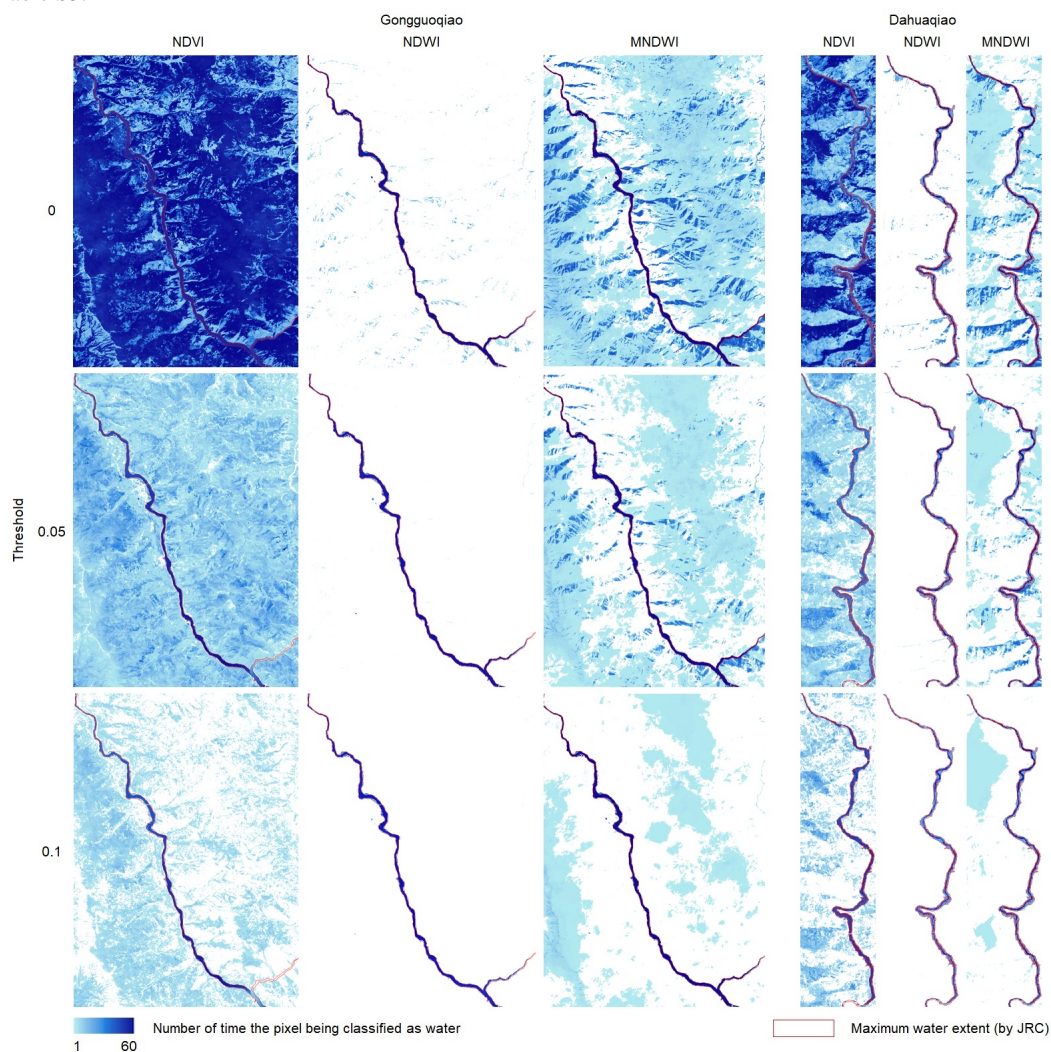


Figure S9. Performance of three spectral indices (NDVI, NDWI, and MNDWI) in extracting the water surface area of Miaowei (left), Huangdeng (middle) and Wunonglong (right) reservoirs. Results are reported for three threshold values, 0, 0.05, and 0.1 and compared to the Maximum Water Extent dataset, developed by the European Commission’s Joint Research Centre (Pekel et al., 2016). The meaning of the three indices is explained in Table S5.

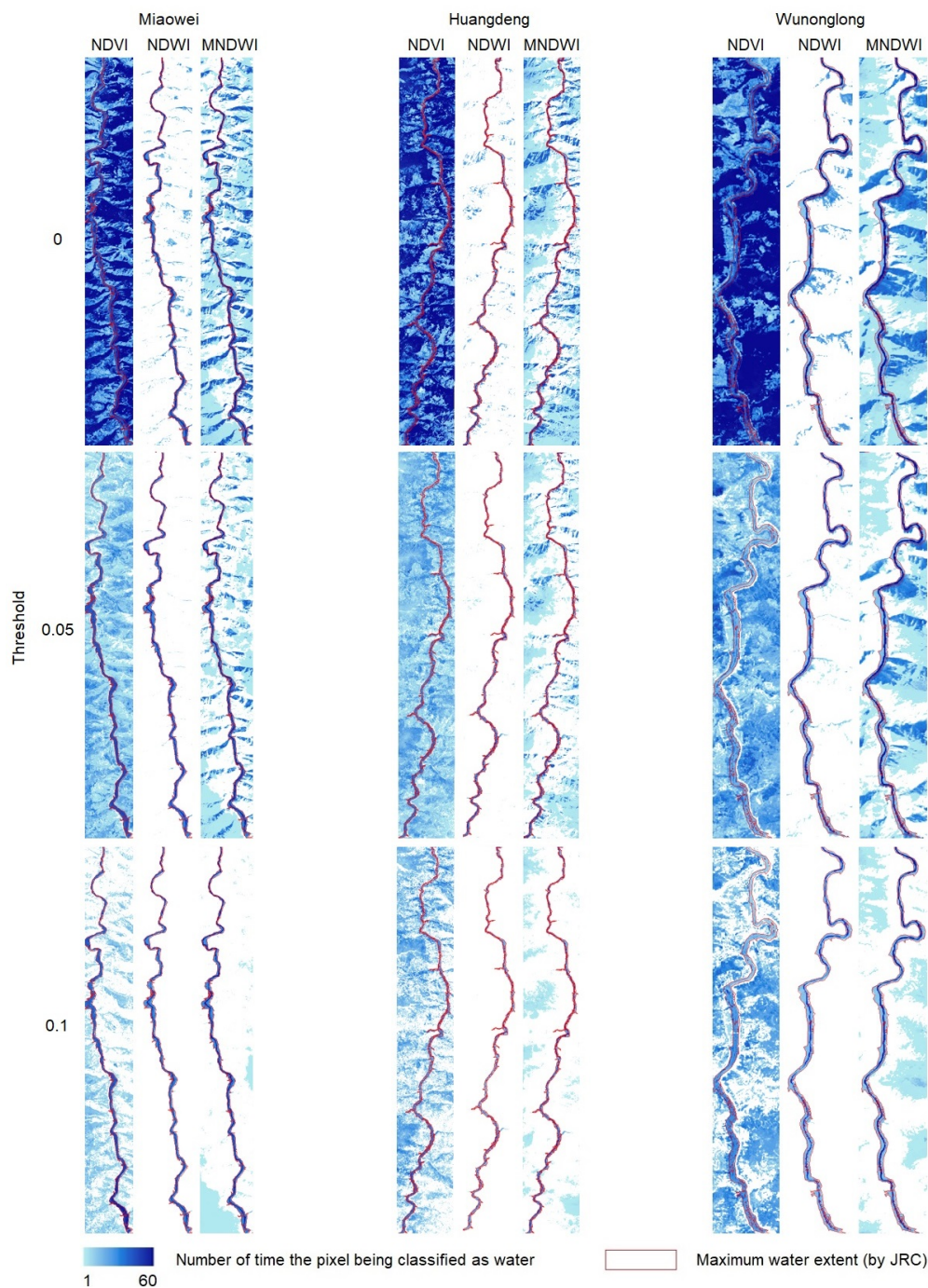


Figure S10. Comparison of the simulated discharge by VIC-Res (blue dots) and observed discharge (grey line) at Chiang Sean for the period 2009-2019 (filling period of Xiaowan and Nuozhadu reservoirs). Observed data are archived from Mekong River Commission (MRC).

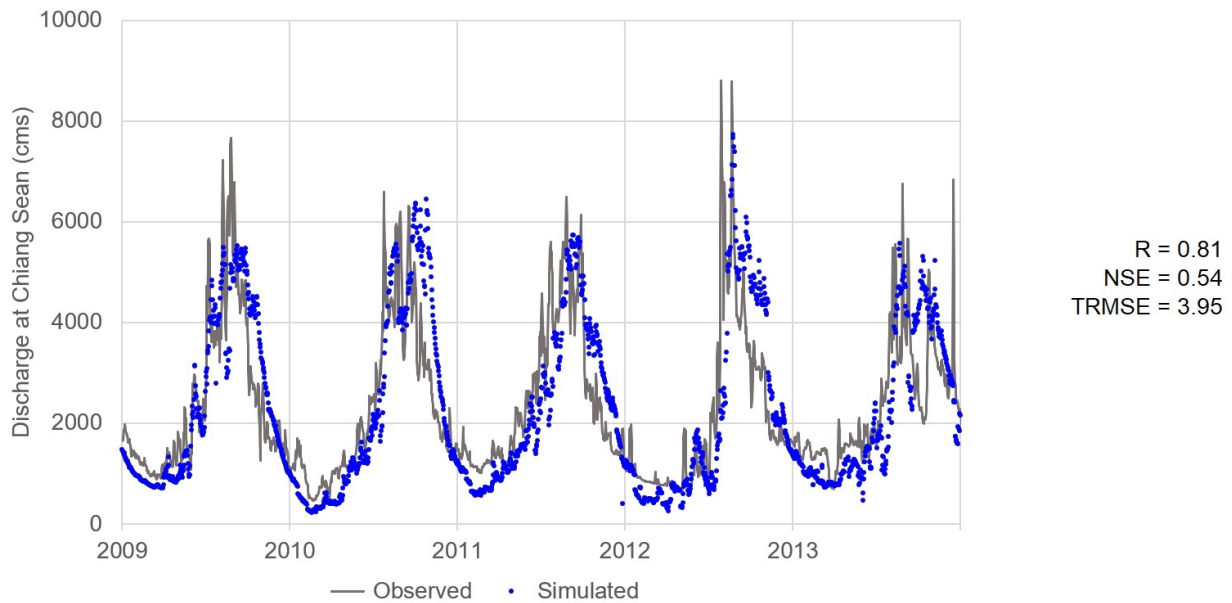


Figure S11. Comparison of storage derived from Landsat images and VIC-Res model for Nuozhadu (left) and Xiaowan (right) reservoirs.

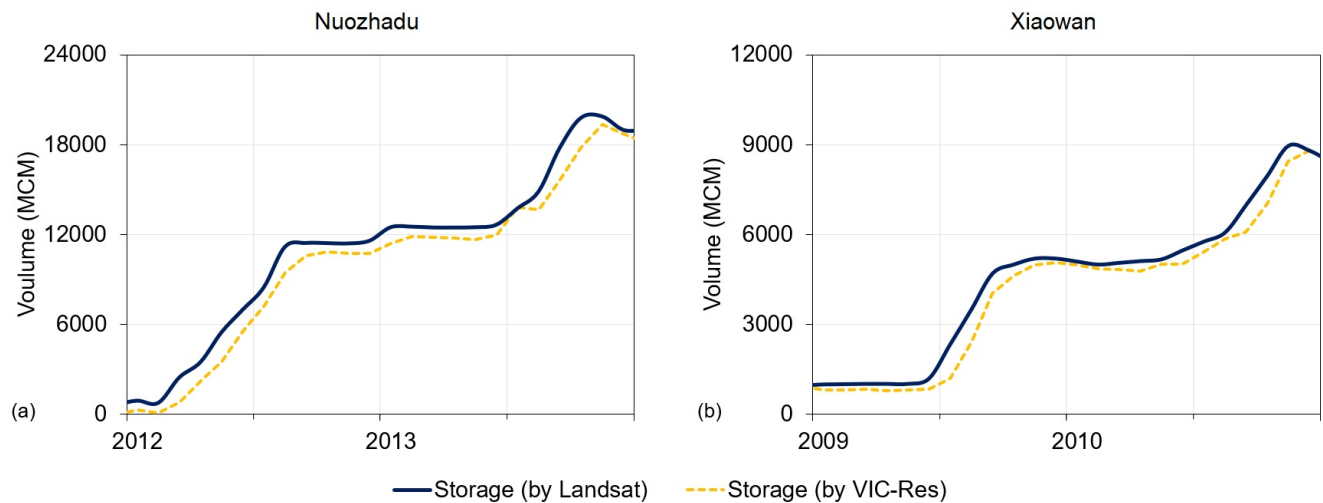


Figure S12. E-A, A-S and E-S curves of Jinghong, Dachaoashan, Manwan and Gongguoqiao reservoir.

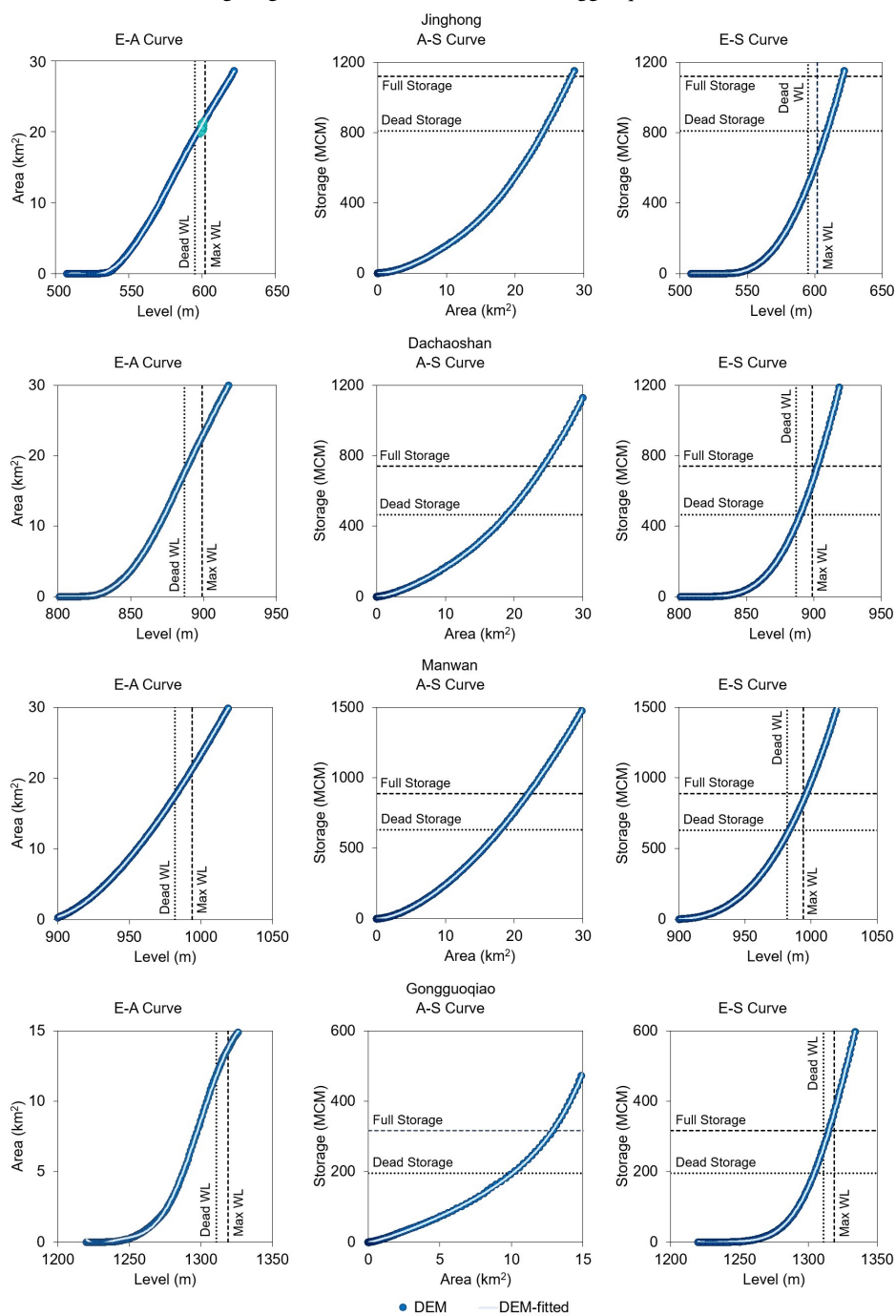


Figure S13. E-A, A-S and E-S curves of Miaowei, Dahuaqiao, Huangdeng and Wunonglong reservoir.

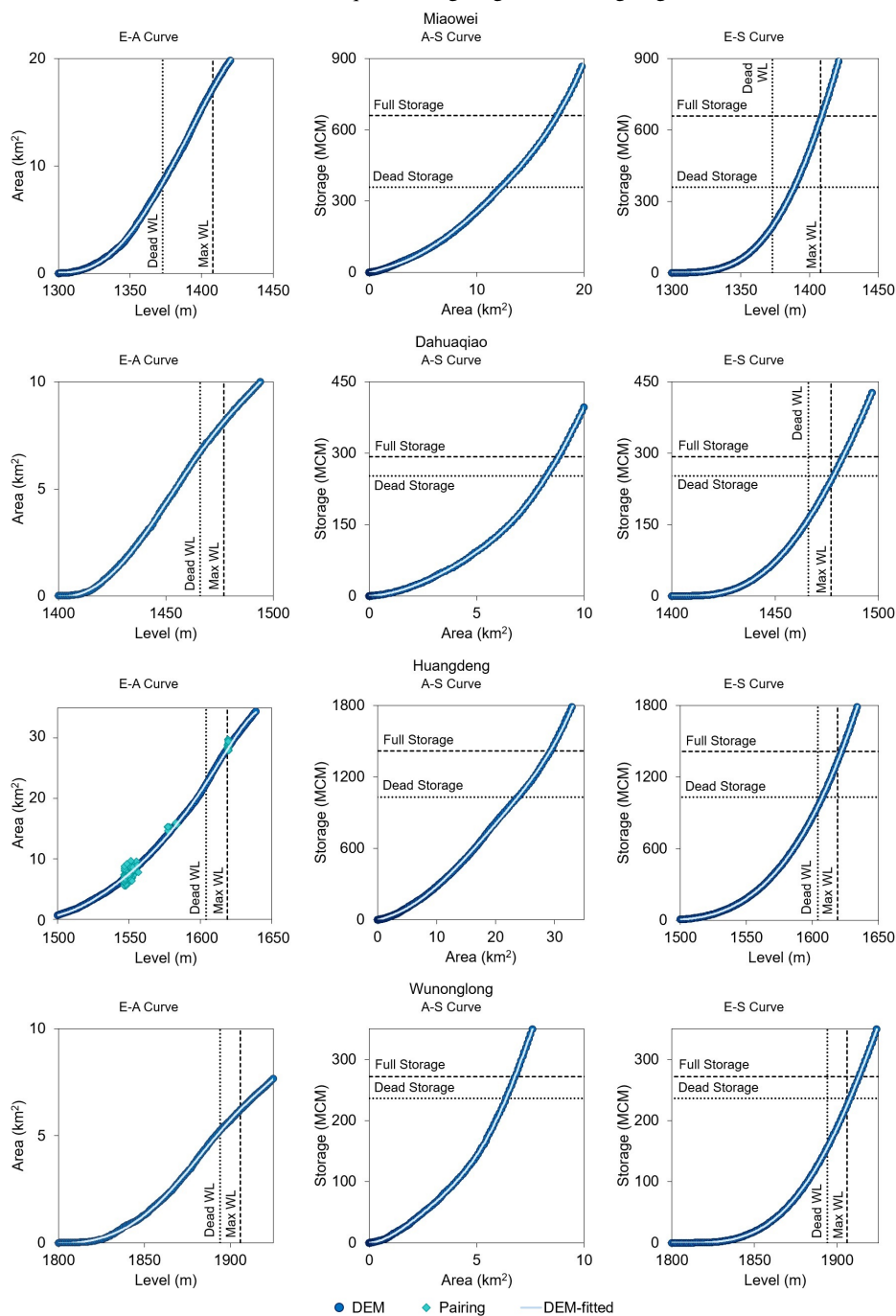


Figure S14. Water surface area of Huangdeng (top) and Jinghong (bottom) reservoirs. Note the drastic difference in WSA values before (lightblue points) and after (cyan points) the classification improvement. The corrected values of WSA are well in agreement with those obtained through altimetry water level data and E-A curves (dark blue points)

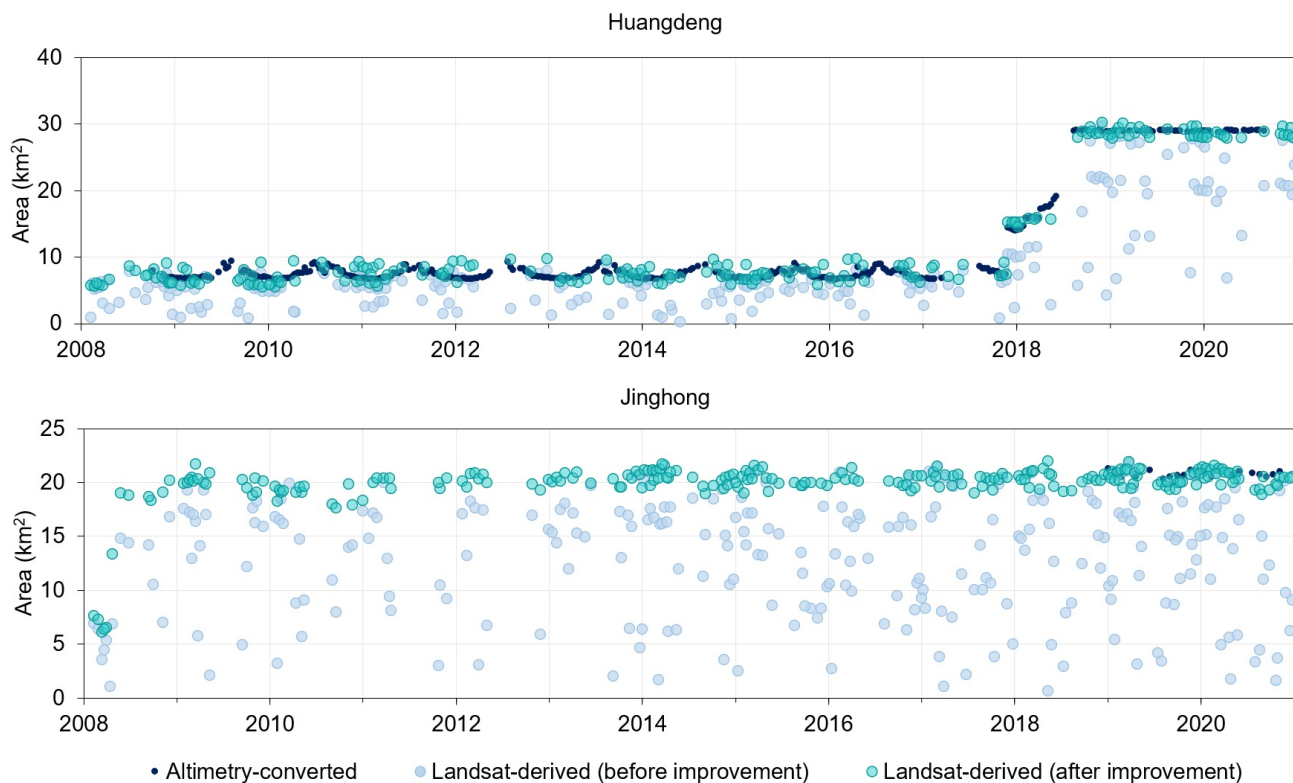


Figure S15. Storage variation of reservoirs on the Lancang River.

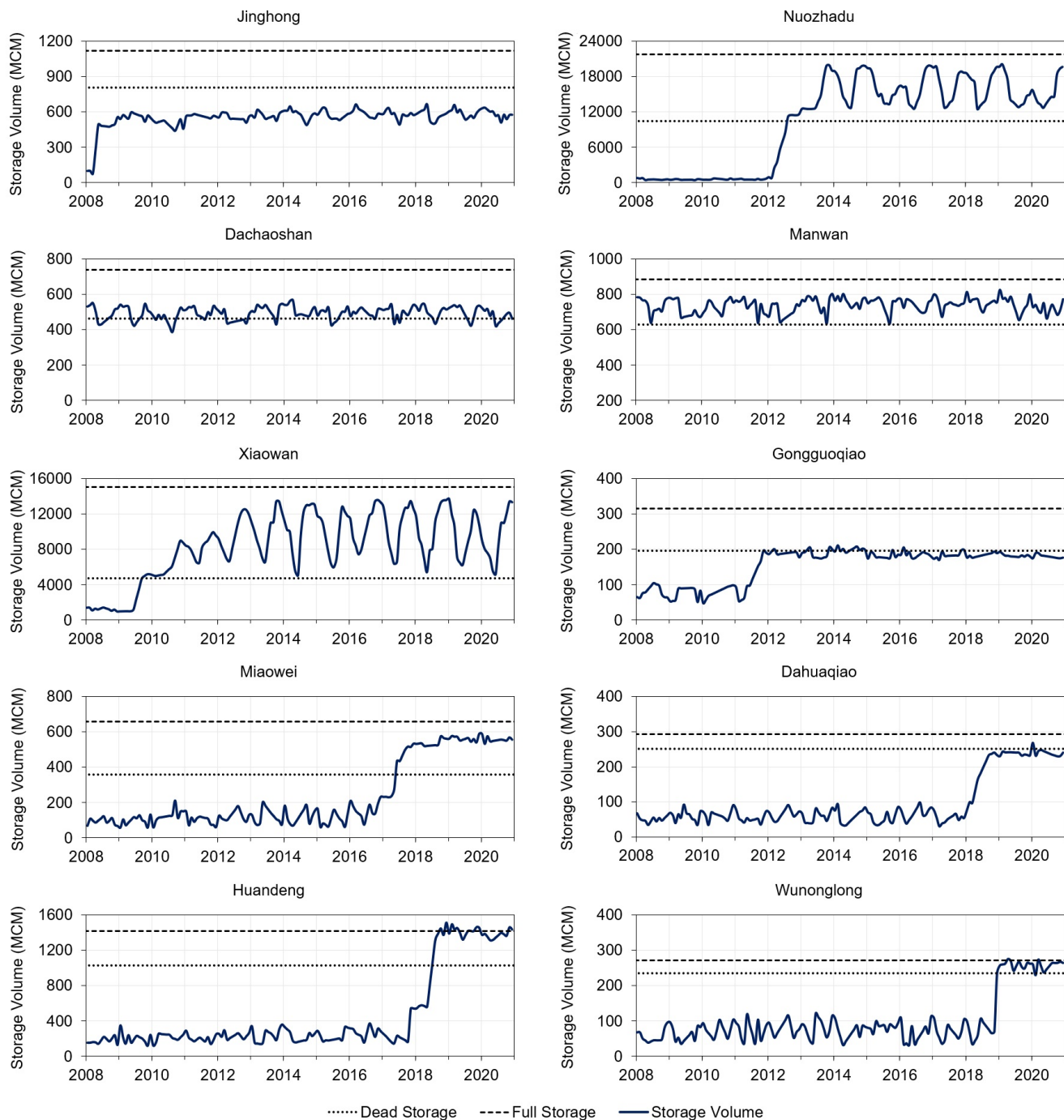


Figure S16. Operation curves of 8 reservoirs (Jinghong, Dachaoshan, Manwan, Gongguoqiao, Miaowei, Dahuaqiao, Huangdeng and Wunonglong).

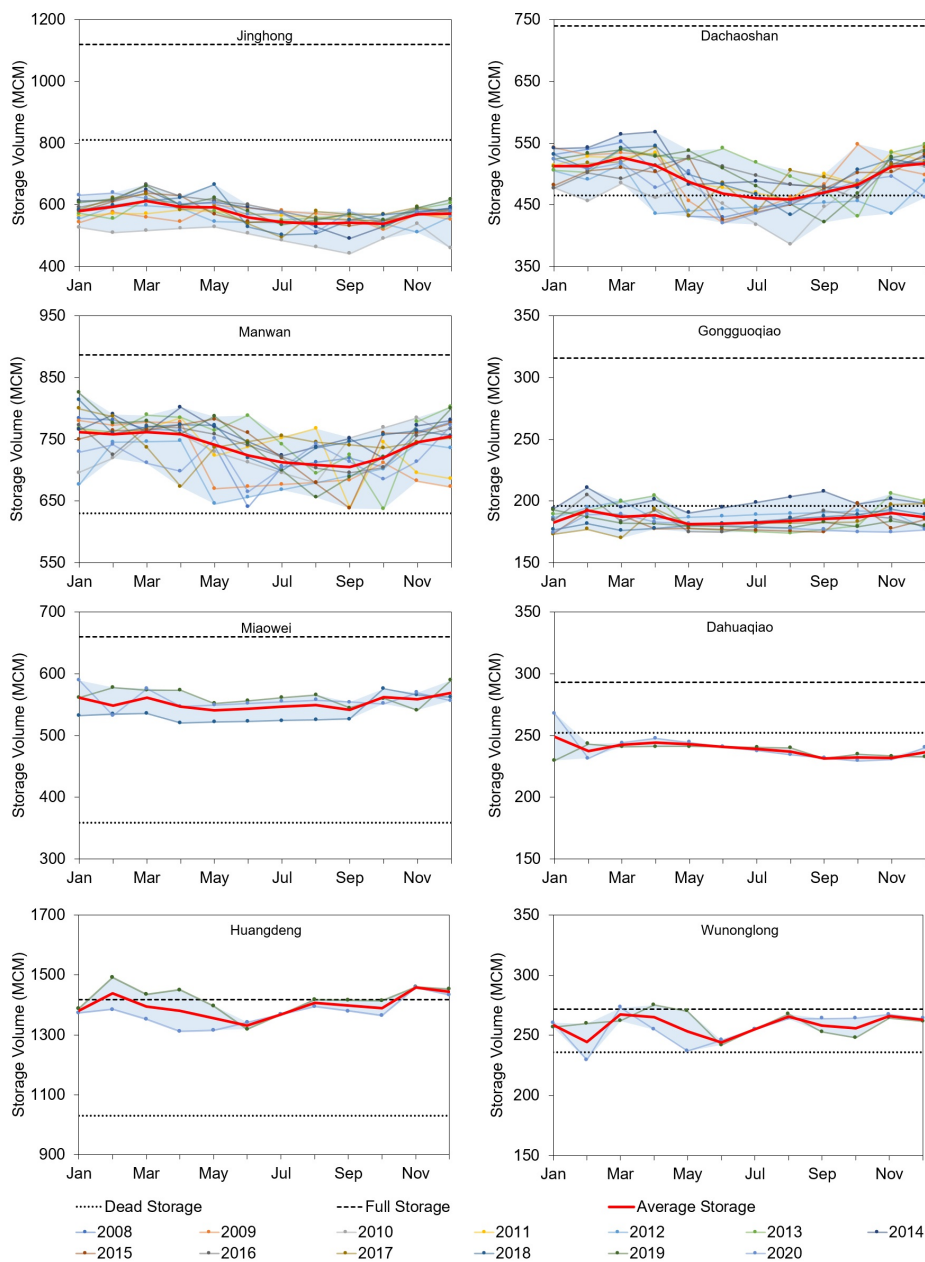
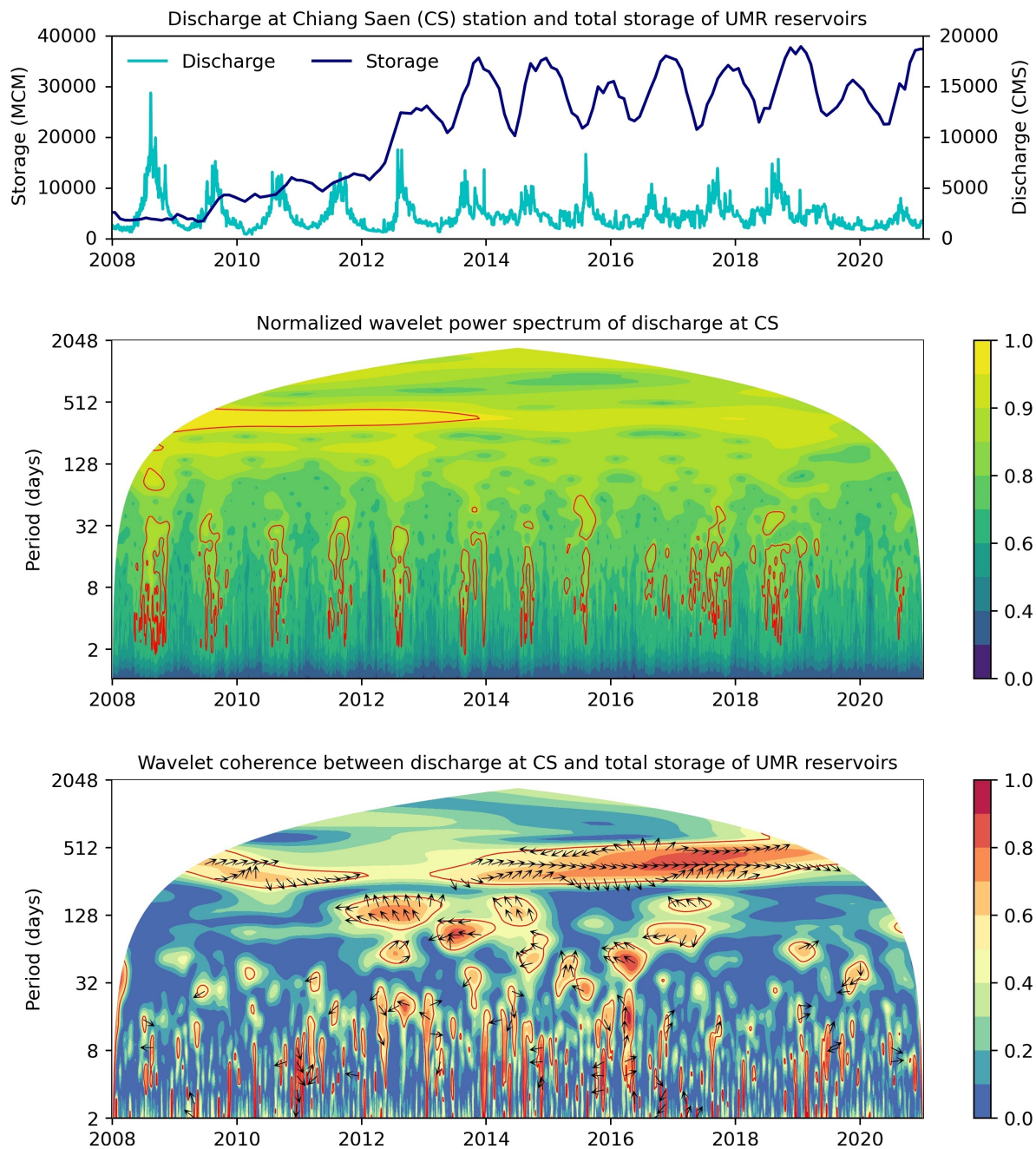


Figure S17. Upper panel: graphical illustration of total storage and discharge at Chiang Saen station. Middle panel: wavelet analysis of the discharge. Colors represent wavelet power, while confidence level contours identify statistically significant power. The flow regime changed in 2014, when Nuozhadu reservoir started its normal operations. Bottom panel: wavelet coherence and phase between discharge and reservoir storage. Contours identify statistically significant coherencies. The vectors indicate the phase difference between discharge and storage.



References

- 20 Bonnama, M. and Hossain, F.: Inferring reservoir operating patterns across the Mekong Basin using only space observations, *Water Resources Research*, 53, 3791–3810, <https://doi.org/10.1002/2016wr019978>, 2017.
- Do, P., Tian, F., Zhu, T., Zohidov, B., Ni, G., Lu, H., and Liu, H.: Exploring synergies in the water-food-energy nexus by using an integrated hydro-economic optimization model for the Lancang-Mekong River Basin, *Science of The Total Environment*, 728, 137 996, <https://doi.org/10.1016/j.scitotenv.2020.137996>, 2020.
- 25 Duan, Z. and Bastiaanssen, W. G. M.: Estimating water volume variations in lakes and reservoirs from four operational satellite altimetry databases and satellite imagery data, *Remote Sensing of Environment*, 134, 403–416, <https://doi.org/10.1016/j.rse.2013.03.010>, 2013.
- Gao, H., Birkett, C., and Lettenmaier, D. P.: Global monitoring of large reservoir storage from satellite remote sensing, *Water Resources Research*, 48, w09 504, <https://doi.org/10.1029/2012wr012063>, 2012.
- Pekel, J.-F., Cottam, A., Gorelick, N., and Belward, A. S.: High-resolution mapping of global surface water and its long-term changes, *Nature*, 540, 418–422, <https://doi.org/10.1038/nature20584>, 2016.
- 30 Zhai, K., Wu, X., Qin, Y., and Du, P.: Comparison of surface water extraction performances of different classic water indices using OLI and TM imageries in different situations, *Geospatial Information Science*, 18, 34–42, <https://doi.org/10.1080/10095020.2015.1017911>, 2015.